MicroRNA-132 mediated loss of p120RasGAP activates endothelium to facilitate pathological angiogenesis

Sudarshan Anand, Bharat K. Majeti, Lisette M. Acevedo, Eric A. Murphy, Rajesh Mukthavaram, Lea Scheppke, Miller Huang, David J. Shields, Jeffrey N. Lindquist, Philip E. Lapinski, Philip D. King, Sara M. Weis and David A. Cheresh

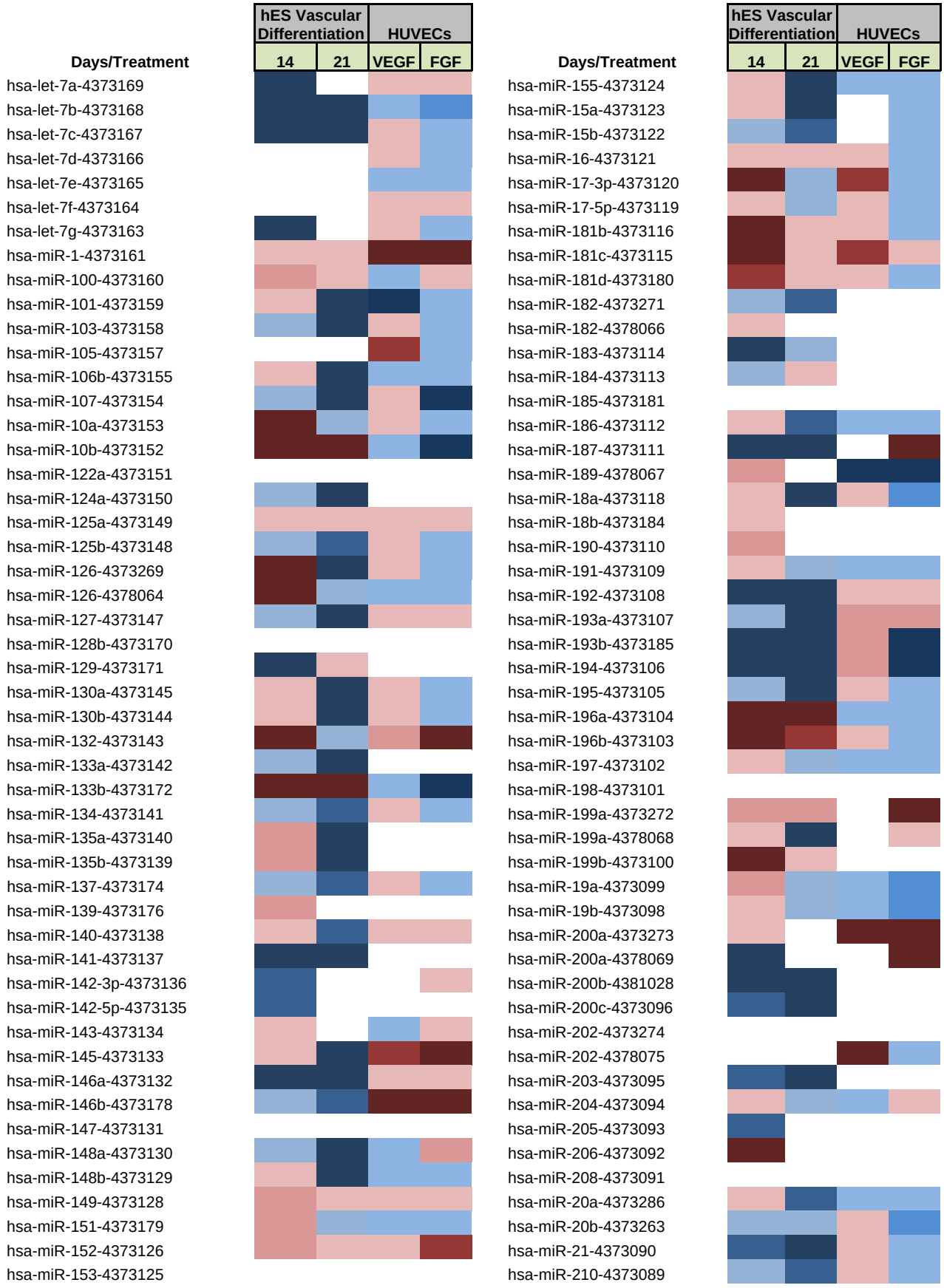

Nature Medicine: doi:10.1038/nm.2186

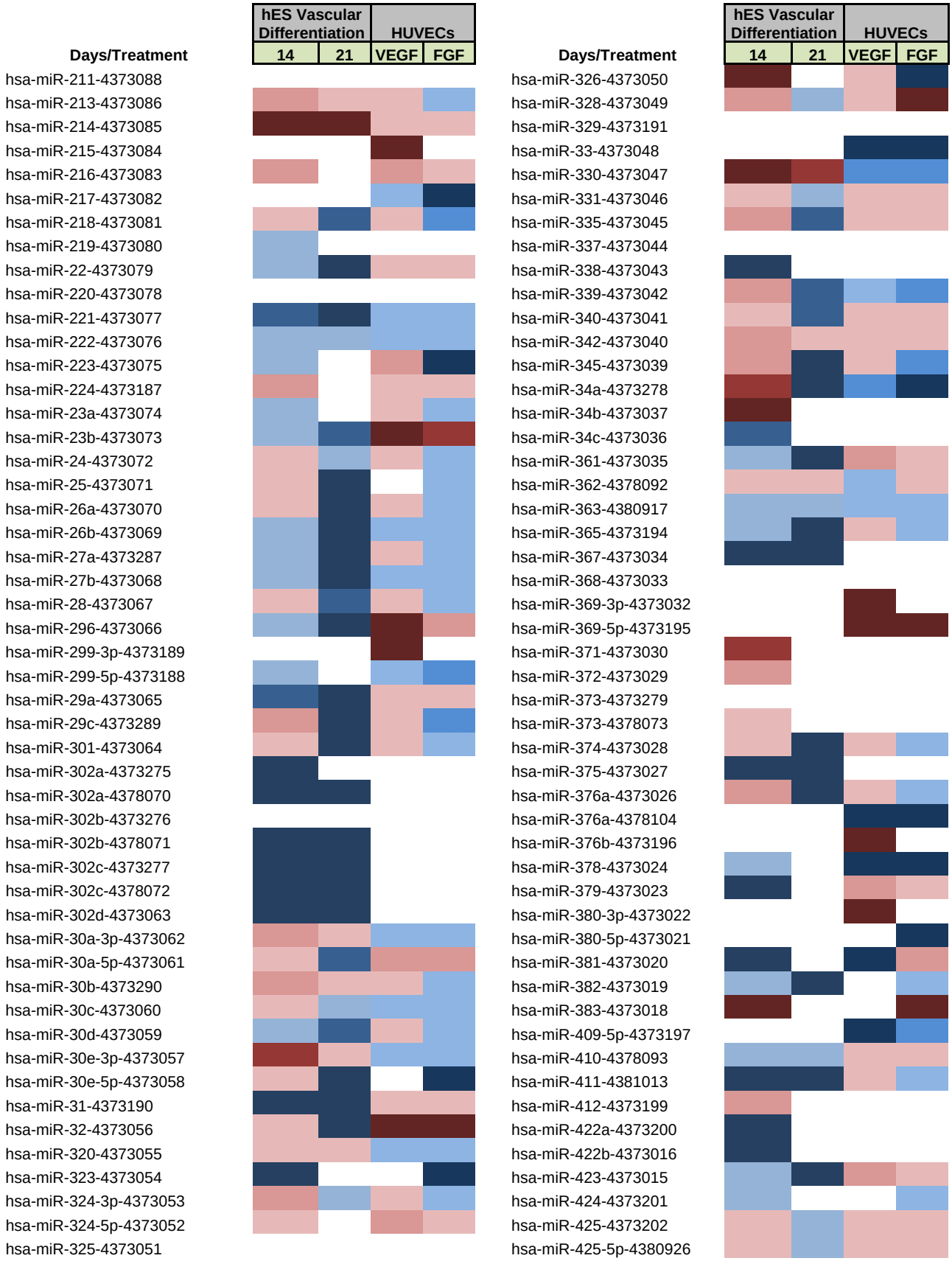
hES Vascular Differentiation
HUVECs
Days/Treatment
14
21
VEGF
FGF
hsa-miR-211-4373088
hsa-miR-213-4373086
hsa-miR-214-4373085
hsa-miR-215-4373084
hsa-miR-216-4373083
hsa-miR-217-4373082
hsa-miR-218-4373081
hsa-miR-219-4373080
hsa-miR-22-4373079
hsa-miR-220-4373078
hsa-miR-221-4373077
hsa-miR-222-4373076
hsa-miR-223-4373075
hsa-miR-224-4373187
hsa-miR-23a-4373074
hsa-miR-23b-4373073
hsa-miR-24-4373072
hsa-miR-25-4373071
hsa-miR-26a-4373070
hsa-miR-26b-4373069
hsa-miR-27a-4373287
hsa-miR-27b-4373068
hsa-miR-28-4373067
hsa-miR-296-4373066
hsa-miR-299-3p-4373189
hsa-miR-299-5p-4373188
hsa-miR-29a-4373065
hsa-miR-29c-4373289
hsa-miR-301-4373064
hsa-miR-302a-4373275
hsa-miR-302a-4378070
hsa-miR-302b-4373276
hsa-miR-302b-4378071
hsa-miR-302c-4373277
hsa-miR-302c-4378072
hsa-miR-302d-4373063
hsa-miR-30a-3p-4373062
hsa-miR-30a-5p-4373061
hsa-miR-30b-4373290
hsa-miR-30c-4373060
hsa-miR-30d-4373059
hsa-miR-30e-3p-4373057
hsa-miR-30e-5p-4373058
hsa-miR-31-4373190
hsa-miR-32-4373056
hsa-miR-320-4373055
hsa-miR-323-4373054
hsa-miR-324-3p-4373053
hsa-miR-324-5p-4373052
hsa-miR-325-4373051
hES Vascular Differentiation
HUVECs
Days/Treatment
14
21
VEGF
FGF
hsa-miR-326-4373050
hsa-miR-328-4373049
hsa-miR-329-4373191
hsa-miR-33-4373048
hsa-miR-330-4373047
hsa-miR-331-4373046
hsa-miR-335-4373045
hsa-miR-337-4373044
hsa-miR-338-4373043
hsa-miR-339-4373042
hsa-miR-340-4373041
hsa-miR-342-4373040
hsa-miR-345-4373039
hsa-miR-34a-4373278
hsa-miR-34b-4373037
hsa-miR-34c-4373036
hsa-miR-361-4373035
hsa-miR-362-4378092
hsa-miR-363-4380917
hsa-miR-365-4373194
hsa-miR-367-4373034
hsa-miR-368-4373033
hsa-miR-369-3p-4373032
hsa-miR-369-5p-4373195
hsa-miR-371-4373030
hsa-miR-372-4373029
hsa-miR-373-4373279
hsa-miR-373-4378073
hsa-miR-374-4373028
hsa-miR-375-4373027
hsa-miR-376a-4373026
hsa-miR-376a-4378104
hsa-miR-376b-4373196
hsa-miR-378-4373024
hsa-miR-379-4373023
hsa-miR-380-3p-4373022
hsa-miR-380-5p-4373021
hsa-miR-381-4373020
hsa-miR-382-4373019
hsa-miR-383-4373018
hsa-miR-409-5p-4373197
hsa-miR-410-4378093
hsa-miR-411-4381013
hsa-miR-412-4373199
hsa-miR-422a-4373200
hsa-miR-422b-4373016
hsa-miR-423-4373015
hsa-miR-424-4373201
hsa-miR-425-4373202
hsa-miR-425-5p-4380926

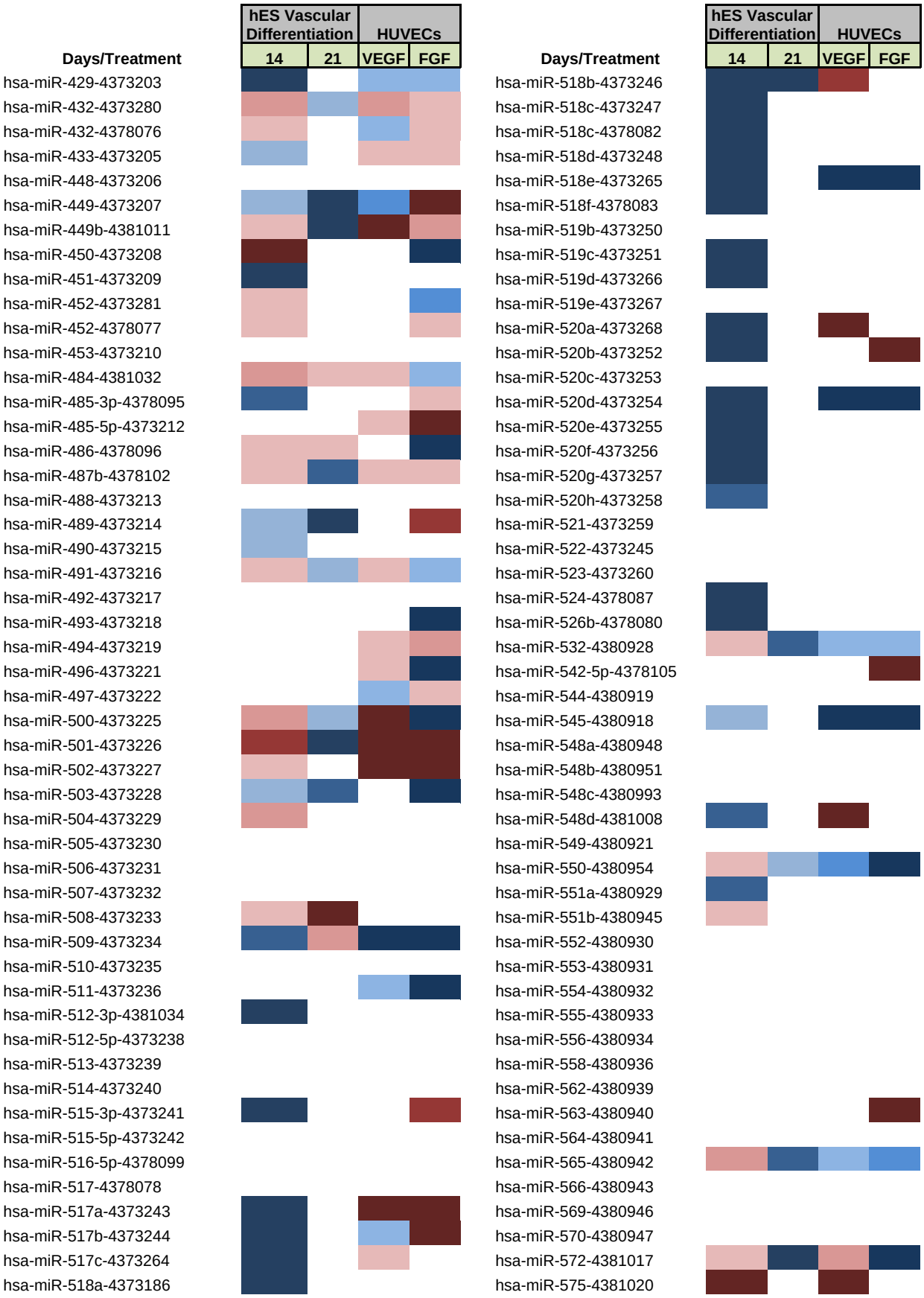

Nature Medicine: doi:10.1038/nm.2186

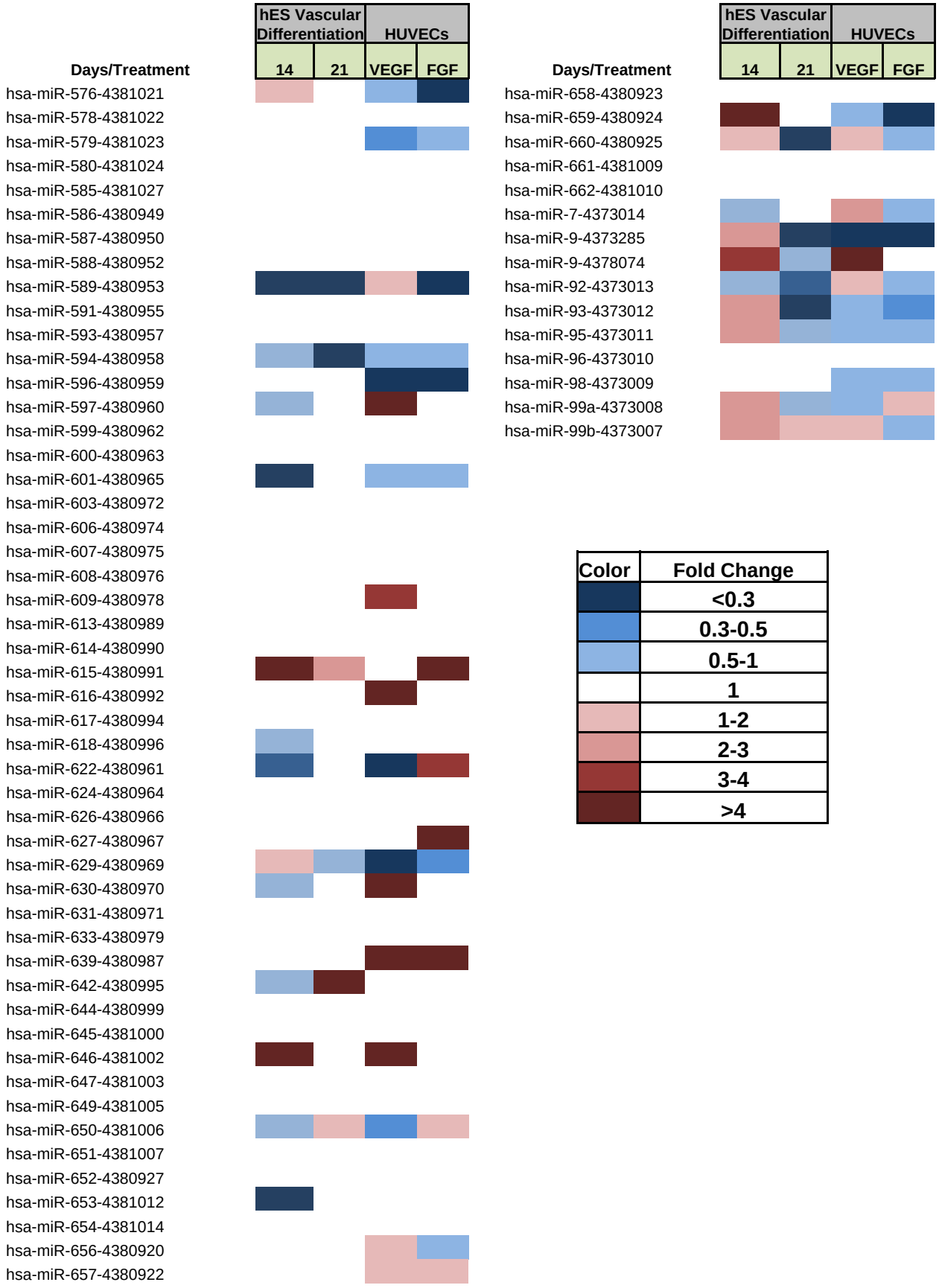

Supplementary Figure 1. Heatmap showing miR profiles of hES cell vascular differentiation at day 14, 21 and HUVECs treated with VEGF and FGF

Nature Medicine: doi:10.1038/nm.2186

microRNA	hES cell vasculogenesis	HUVEC VEGF/FGF	Combined Rank
miR-132	8	19	1
miR-501	27	1	2
miR-181c	20	26	3
miR-646	14	40	4
miR-575	18	43	5

Supplementary Figure 2. Ranking of miRs in angiogenesis screens.
The raw Ct (Cycle threshold) values from the TaqMan panel were filtered to include only Ct values below 32 to eliminate false positives based on the manufacturer's recommendation. miR fold upregulation was calculated on the basis of miR Ct values compared to the Ct values of the housekeeping small RNA RNU48. The miRs were ranked according to their fold upregulation compared to the untreated control for HUVECs and day 0 values for hES differentiation. Combined Rank was obtained by averaging the rank of both the hES cell and HUVEC screens.

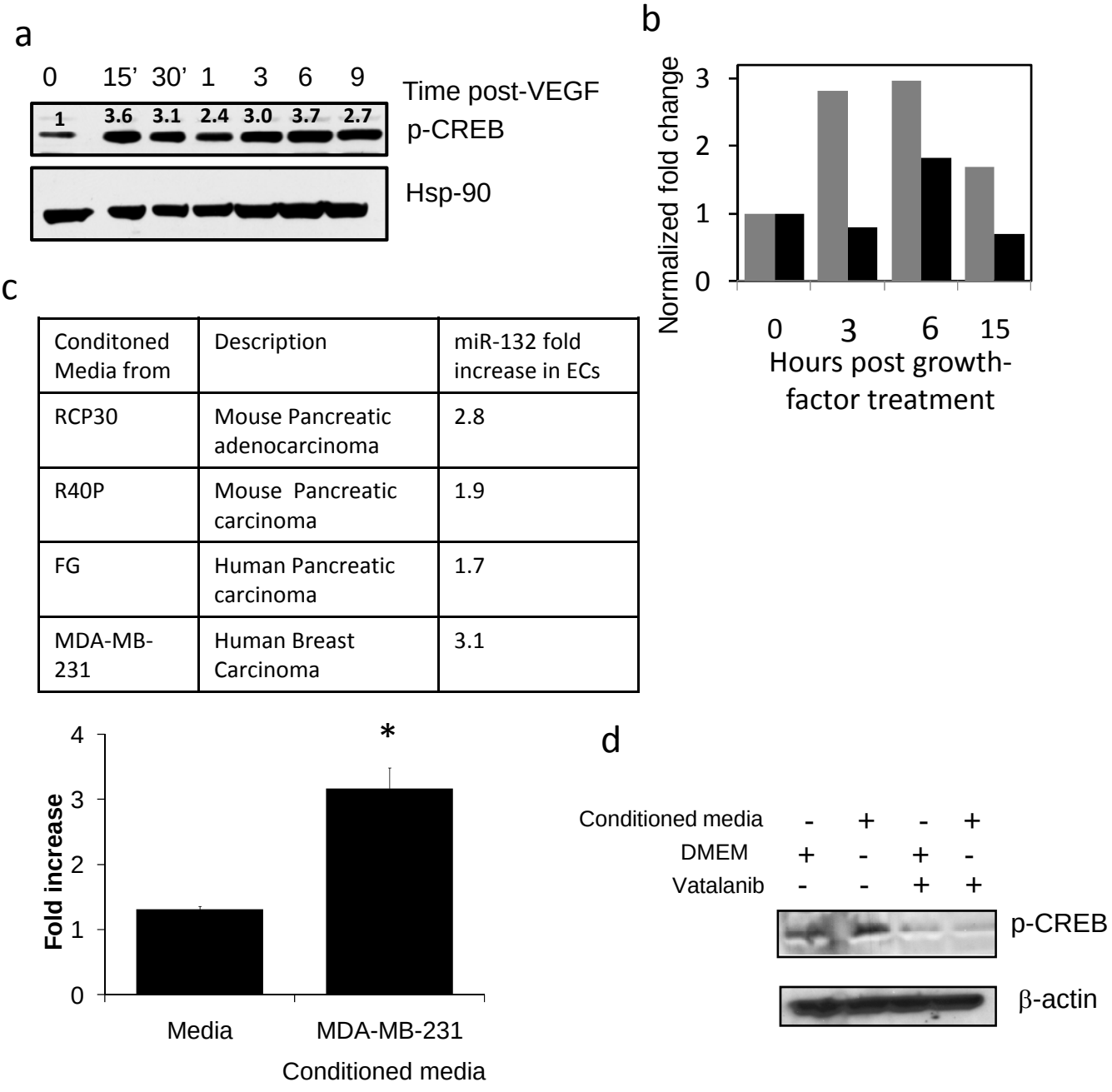

Conditoned Media from	Description	miR-132 fold increase in ECs
RCP30	Mouse Pancreatic adenocarcinoma	2.8
R40P	Mouse Pancreatic carcinoma	1.9
FG	Human Pancreatic carcinoma	1.7
MDA-MB-231	Human Breast Carcinoma	3.1

Supplementary Figure 3. miR-132 is rapidly upregulated upon growth factor treatment in HUVECs. (a) HUVECs were starved overnight and treated with 40 ng/ml recombinant human VEGF-165. At the indicated time points the cells were harvested lysed and assayed for phosphorylation of CREB (Ser133). The numbers indicate band intensities relative to 0 hour. **(b)** HUVECs were starved overnight and treated with either 40ng/ml recombinant human VEGF-165 (grey bars) or 100 ng/ml bFGF (black bars). RNA was isolated and RT-PCR was performed at the indicated time points. Bars reflect mean change of miR-132 levels normalized to the expression of the housekeeping small RNA RNU-48. **(c)** HUVECs were starved overnight and treated with either complete DMEM or conditioned DMEM from tumors and RT-PCR was performed as described in (b). (d) HUVECs were starved overnight and treated with Vatalanib or vehicle for 30 minutes and subsequently either conditioned media or DMEM was added. 15 minutes later the cells were lysed and assayed for phosphorylated CREB.

Nature Medicine: doi:10.1038/nm.2186

a

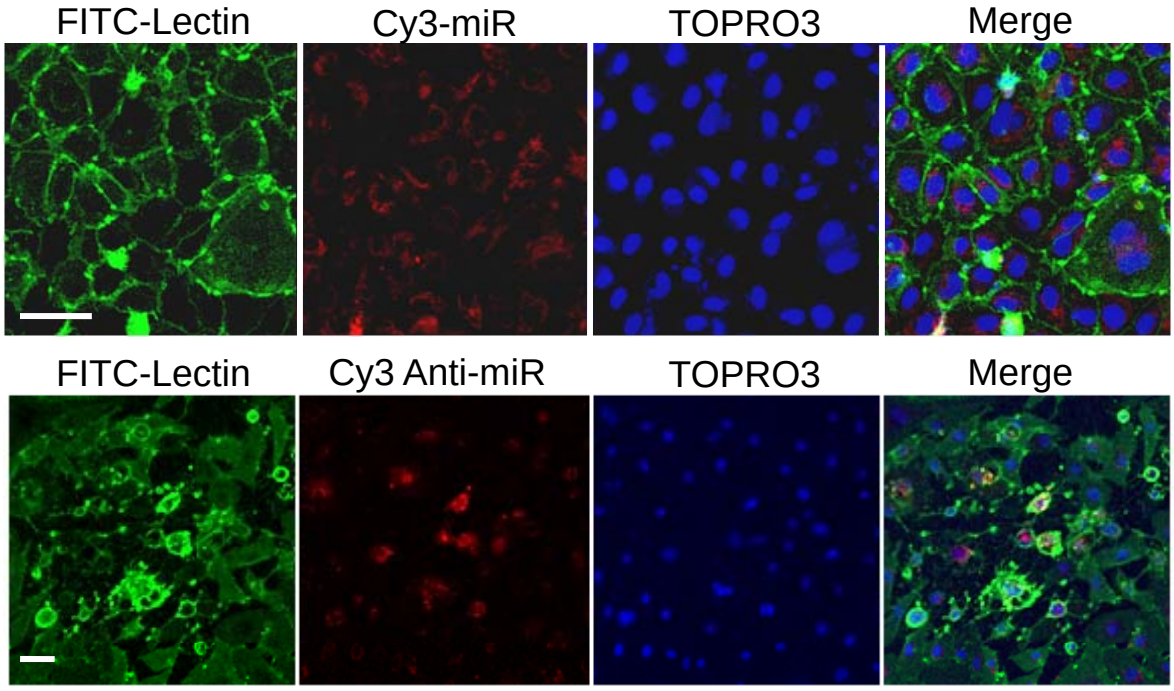

b

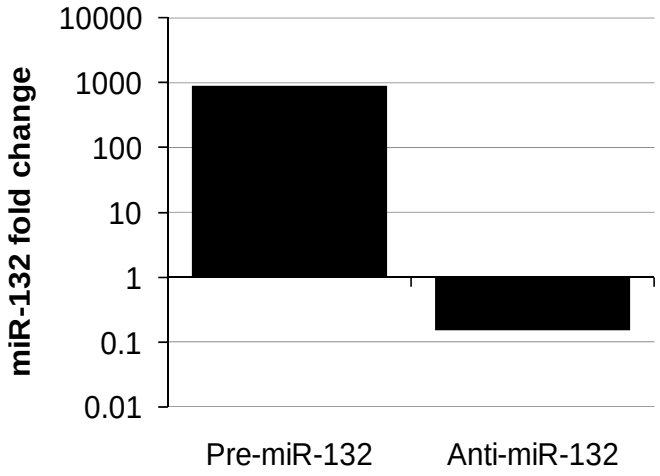

Supplementary Figure 4. Expression and knockdown of miR-132 in HUVECs. (a) Representative confocal image of FITC-lectin labeled HUVECs transfected with 30nM Cy3-labeled miR or anti-miR showing the perinuclear localization of miR or anti-miR. Scale bar = 50μm **(b)** HUVECs were transfected with 30nM control miR or miR-132 or control anti-miR or anti-miR-132. 48 hours later the cells were harvested and RT-PCR was performed. Fold change with respect to RNU48 is shown. One of three independent experiments is shown.

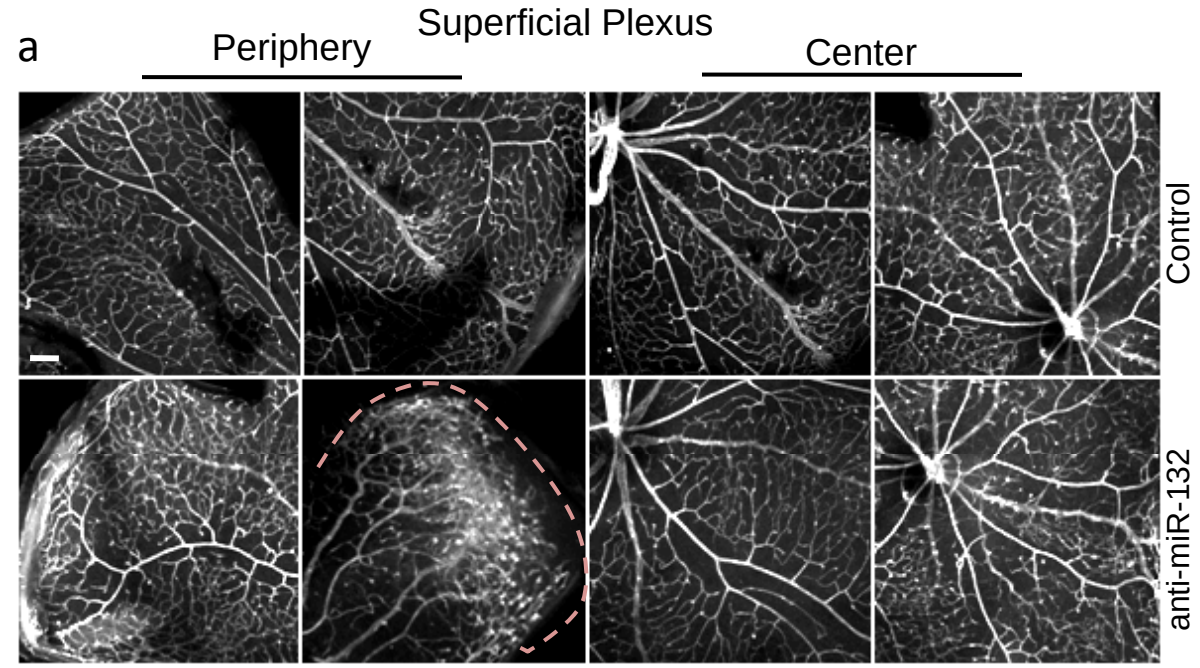

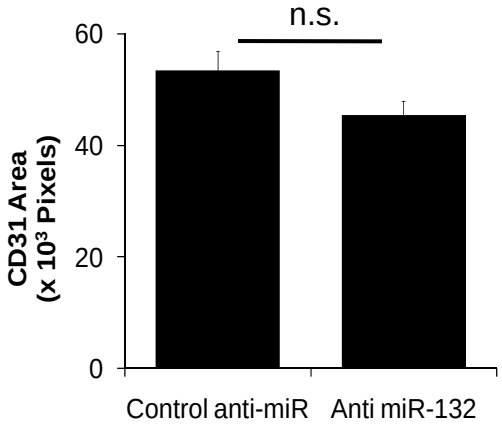

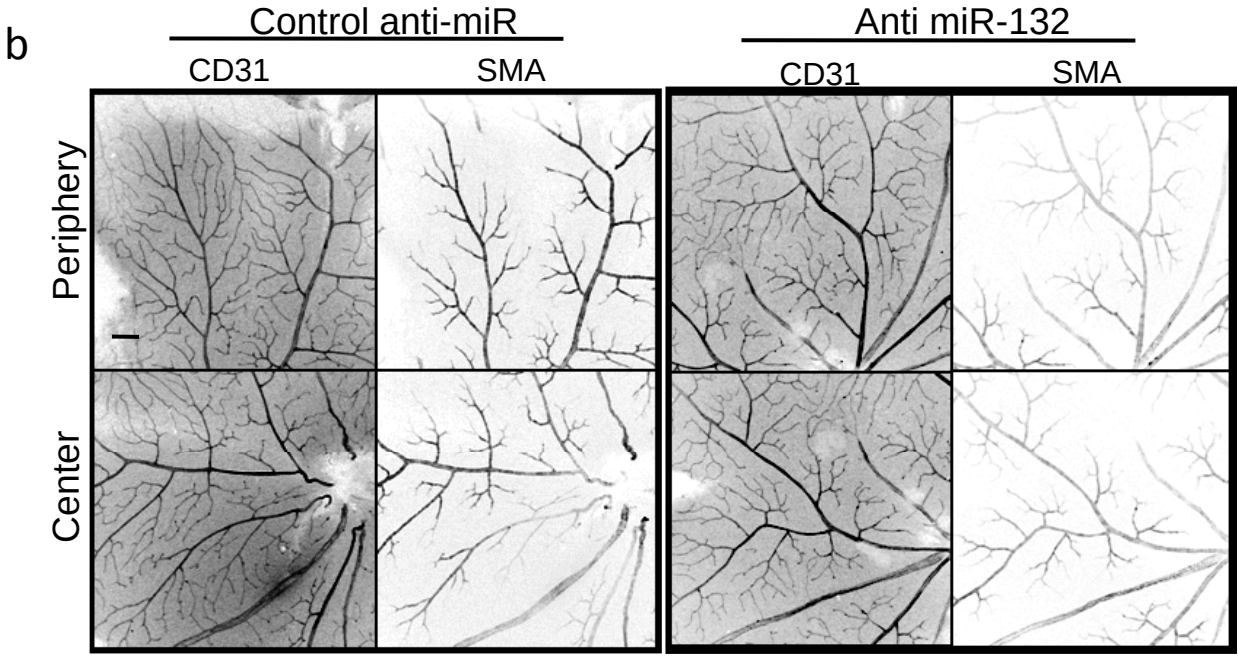

Nature Medicine: doi:10.1038/nm.2186

Supplementary Figure 5. Anti-miR-132 has minimal effect on established vasculature in the retina. a) Representative images of the superficial plexus from P12 retinas of mice injected with either a control anti-miR or Anti miR-132 and stained with CD31-FITC. Bar graph depicts mean + s.e.m of CD31 area as measured by pixel intensity. **b)** Representative images from retinas of adult mice stained with CD31 and SMA. Scale Bar = 100 microns

a

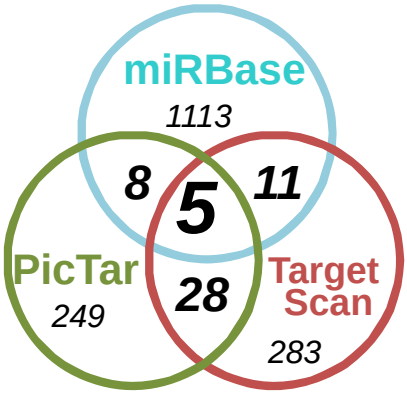

b

Rank		Alternative names	Binding Energy (kcal/mol)	Synergistic sites
1	RasGAP	Rasa1, p120RasGAP	-23.0 and -21.1	Yes
2	TMEFF1	tomoregulin-1	-22.6	No
3	LRRFIP1	GCF2, TRIP	-20.4	No
4	ZNF644	zinc-finger protein 644	-19.8	No
5	TIMM9	TIM9	-17.2	No

c

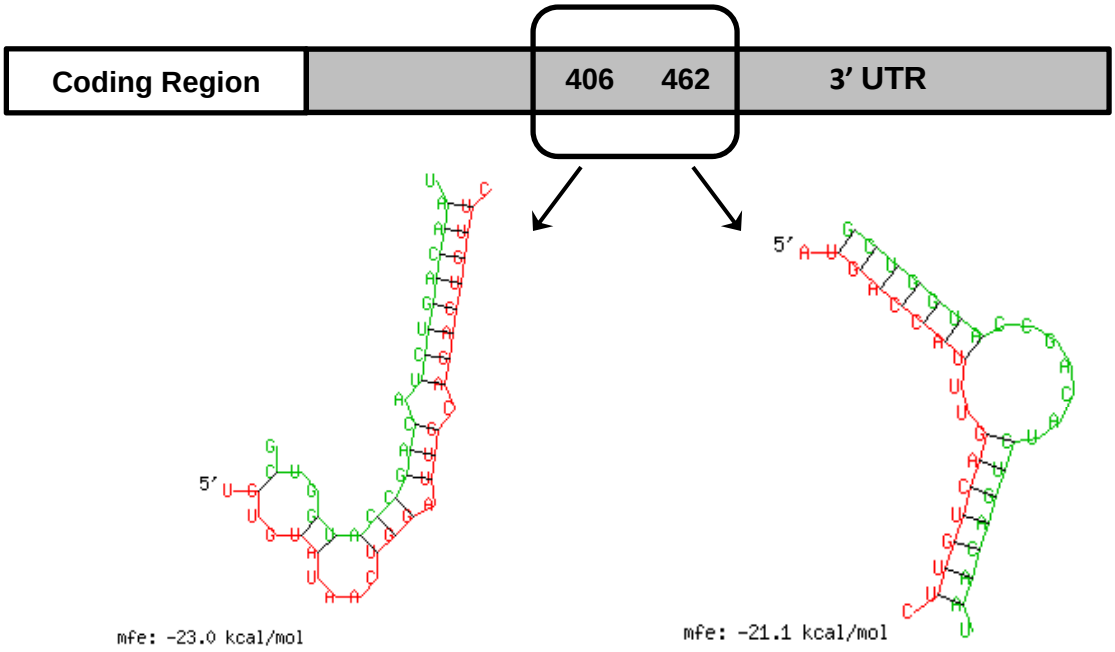

d

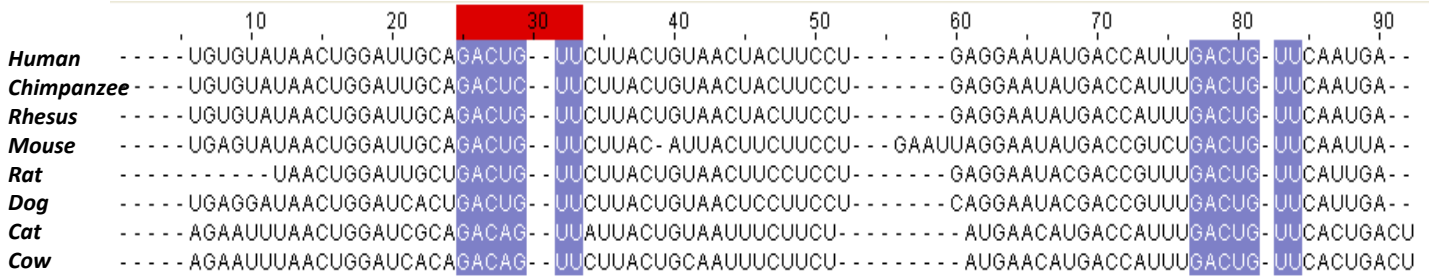

Supplementary Figure 6. In silico identification of p120RasGAP as a putative miR-132 target.(a) Venn diagram of the predictions of human miR-132 targets by three different algorithms yielding 5 common hits. **(b)** Ranking of the 5 common targets based on the RNA hybrid scores and presence of synergistic sites[17]. **(c)** Schematic illustration of RNAhybrid models showing binding of miR-132 (green) with human p120RasGAP 3' untranslated region (UTR). **(d)** p120RasGAP 3'UTR sequences from different species showing a high degree of homology. Shaded regions represent the binding site of the miR-132 seed sequences

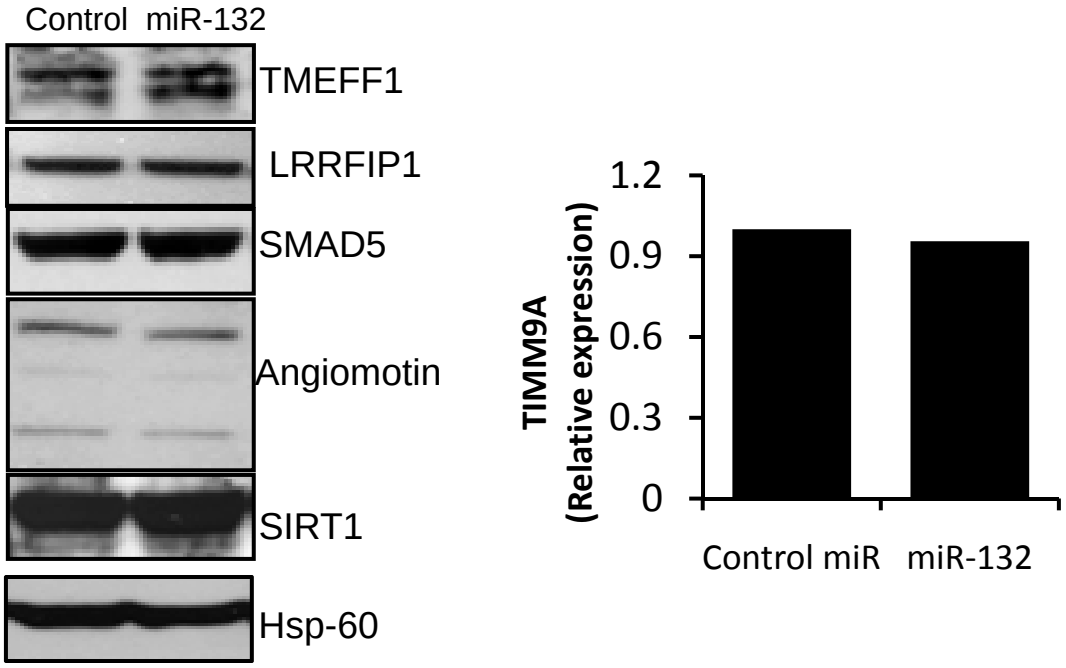

Supplementary Figure 7. miR-132 transfection does not downregulate some of the top predicted targets. HUVECs were transfected with either a control miR or miR-132. 48 hours later the cells were lysed and the lysates were blotted for the indicated proteins (left panel) or RNA was isolated and RT-PCR was performed as described. The levels of TIMM9A were normalized to β–actin.

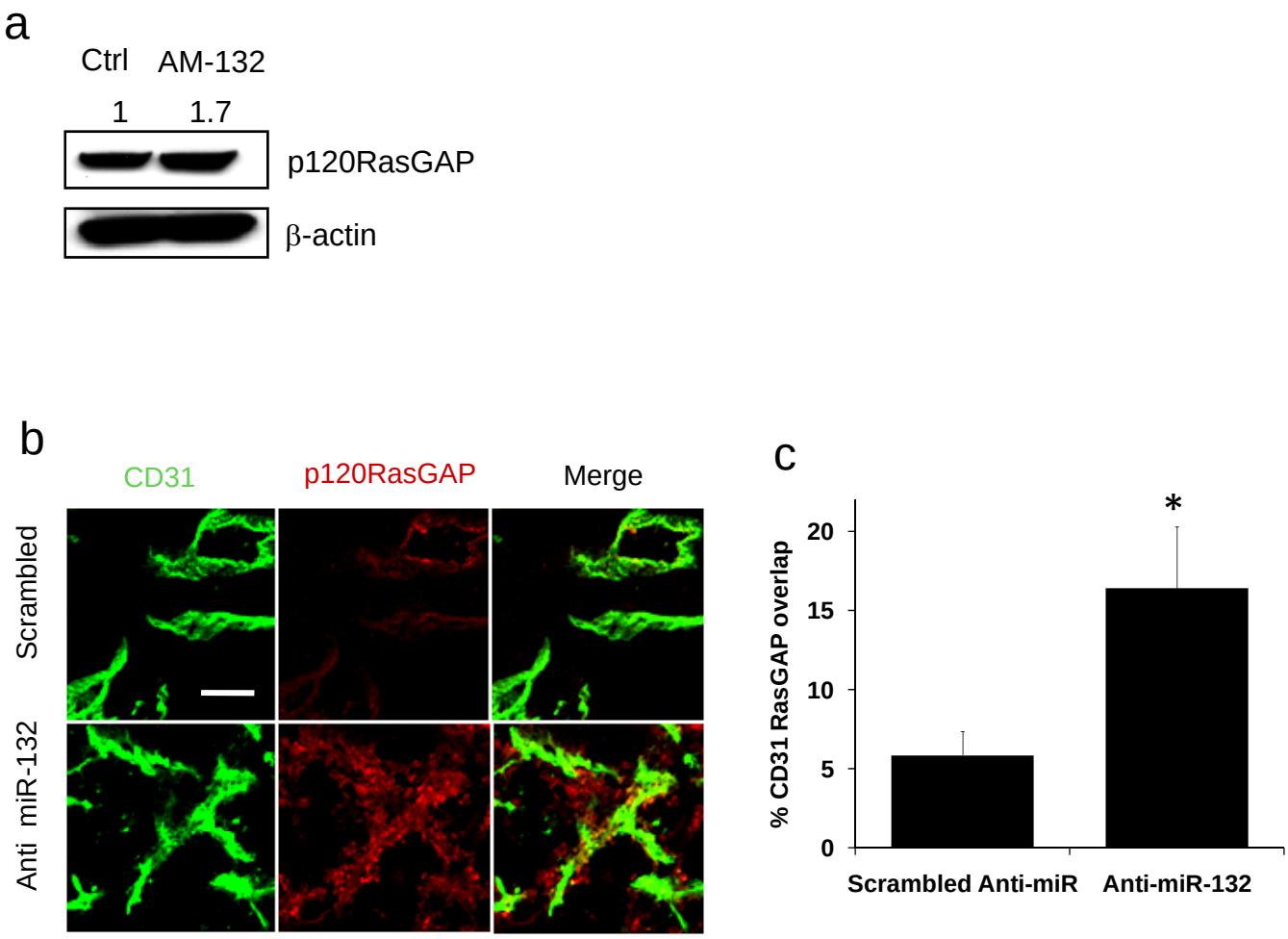

Supplementary Figure 8. Anti-miR-132 upregulates p120RasGAP in vitro and in vivo. **(a)** HUVECs were transfected with either scrambled control anti-miR or 30nM anti-miR-132 and assayed for p120RasGAP expression. Numbers indicate fold increase normalized to loading control. **(b)** and **(c)** B6 mice were injected with bFGF containing matrigel plugs. On day 3 and day 4, mice were injected i.v. with either 20 μg of scrambled anti-miR or anti-miR-132. Mice were euthanized on day 5 and the plugs were harvested. Representative confocal images (b) and mean % overlap between CD31 and p120RasGAP (c) is shown. n=3 mice per group. Scale bar = 50 μm.

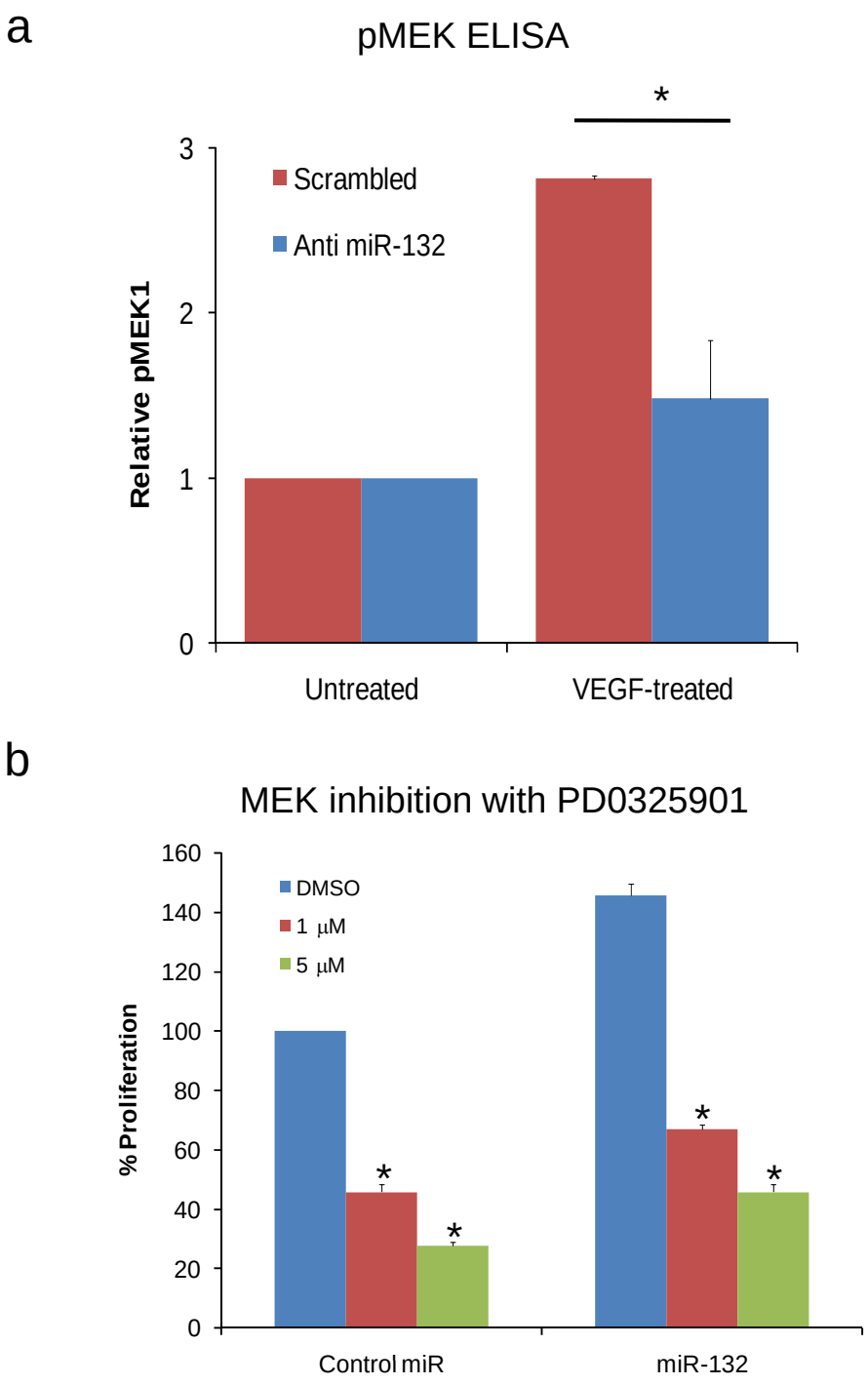

Supplementary Figure 9. miR-132 functions through the regulation of the MEK pathway in HUVECS. a) HUVECs were transfected with either a control anti-miR or anti miR-132. 24 hours later, the cells were starved overnight and treated with recombinant human VEGF-165 (50 ng/ml). 10 minutes later the cells were lysed and pMEK levels were measured using a Pathscan ELISA kit. Mean + s.e.m. of duplicate samples are shown. **b)** HUVECs were transfected with either a control miR or miR-132 in serum free media. 24 hours later the cells were treated with a MEK inhibitor at the indicated concentrations and 30 minutes later treated with 50 ng/ml recombinant humanVEGF-165. Subsequently the cells were pulsed with BrdU and the proliferation was measured using a BrdU ELISA.

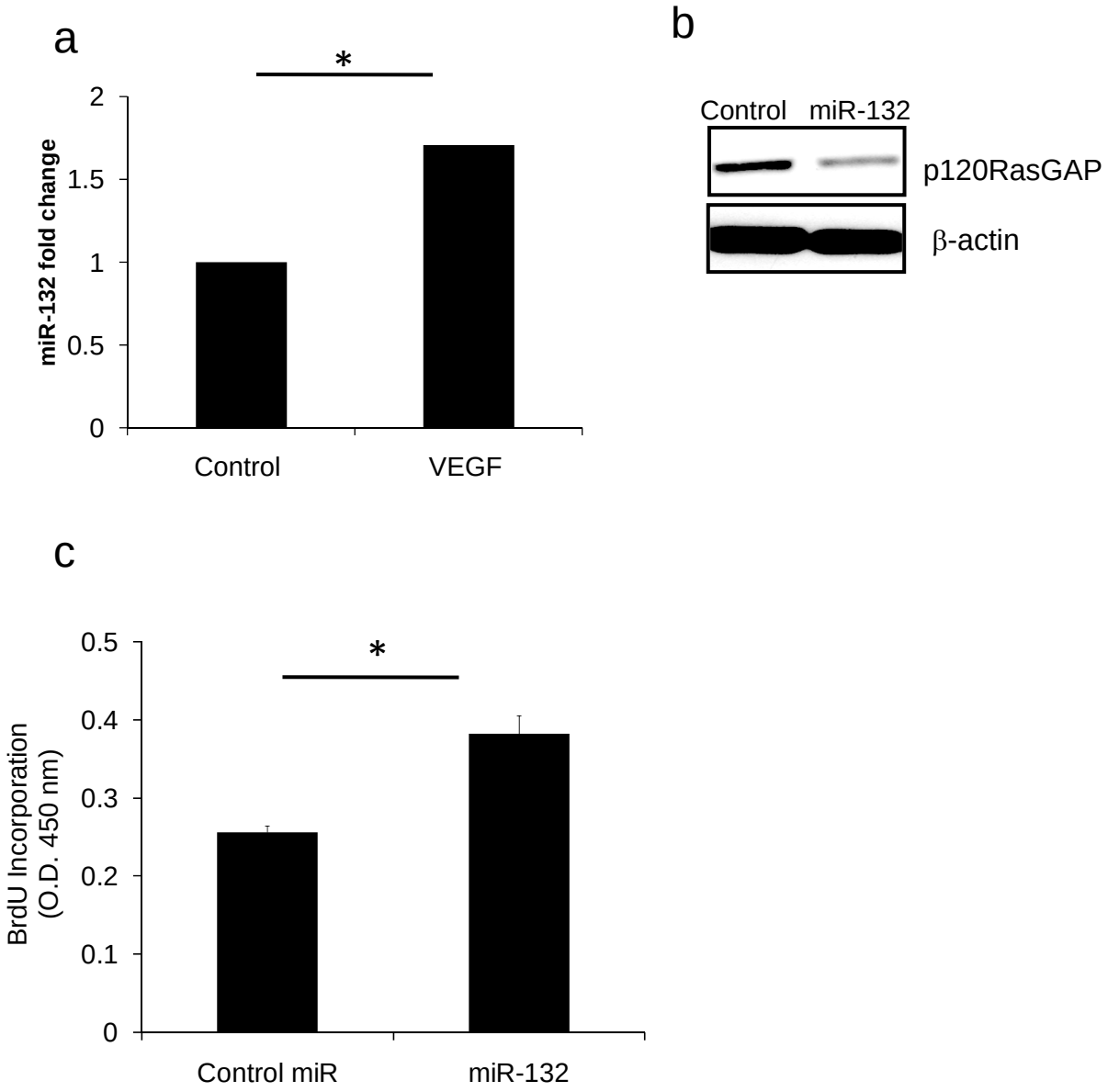

Supplementary Figure 10. miR-132 regulates p120RasGAP in mouse endothelioma cells. (a) b.End3 cells were starved overnight and stimulated with 50 ng/ml recombinant human VEGF-165. RNA was isolated 6 hours later and RT-PCR was performed for miR-132 and snoRNA202. miR-132 levels normalized to snoRNA202 are shown. (b) b.End3 cells were transfected with 50 nM control miR or miR-132. 48 hours later, the cells were lysed and probed for p120RasGAP expression by western blot. (c) b.End3 cells were transfected as in (b) and proliferation was measured 48 hours later by BrdU incorporation. Bars show mean + s.e.m. * $P<0.05$

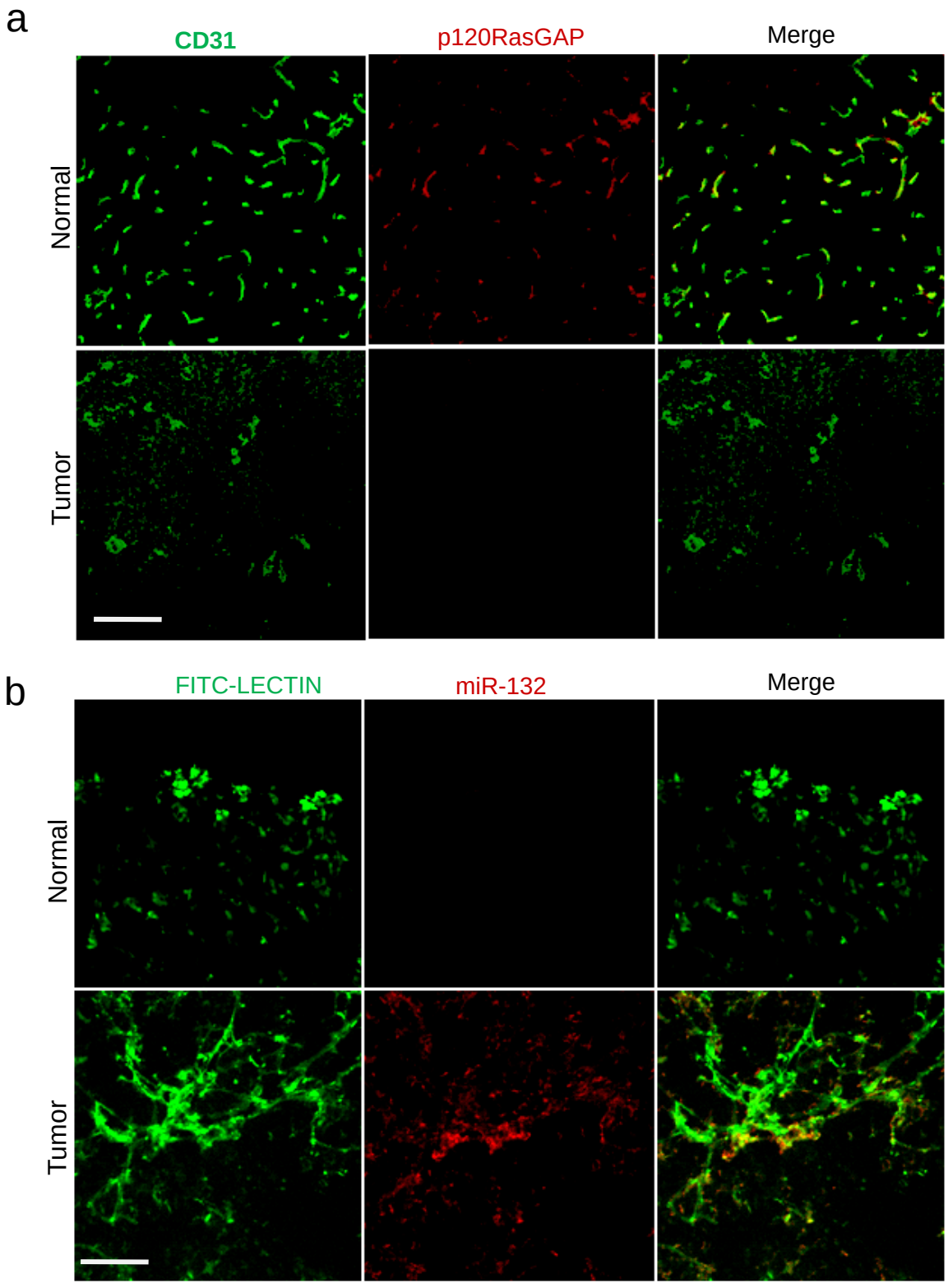

Supplementary Figure 11. Reciprocal expression of miR-132 and p120RasGAP on tumor endothelium vs normal endothelium. Tissue sections from a normal mouse pancreas or an orthotopic pancreatic carcinoma stained with CD31 and p120RasGAP **(a)** or stained for miR-132 expression by in situ hybridization **(b).** One representative image of atleast three mice is shown. Scale bar (a) = 100 microns, (b) = 25 microns.

a

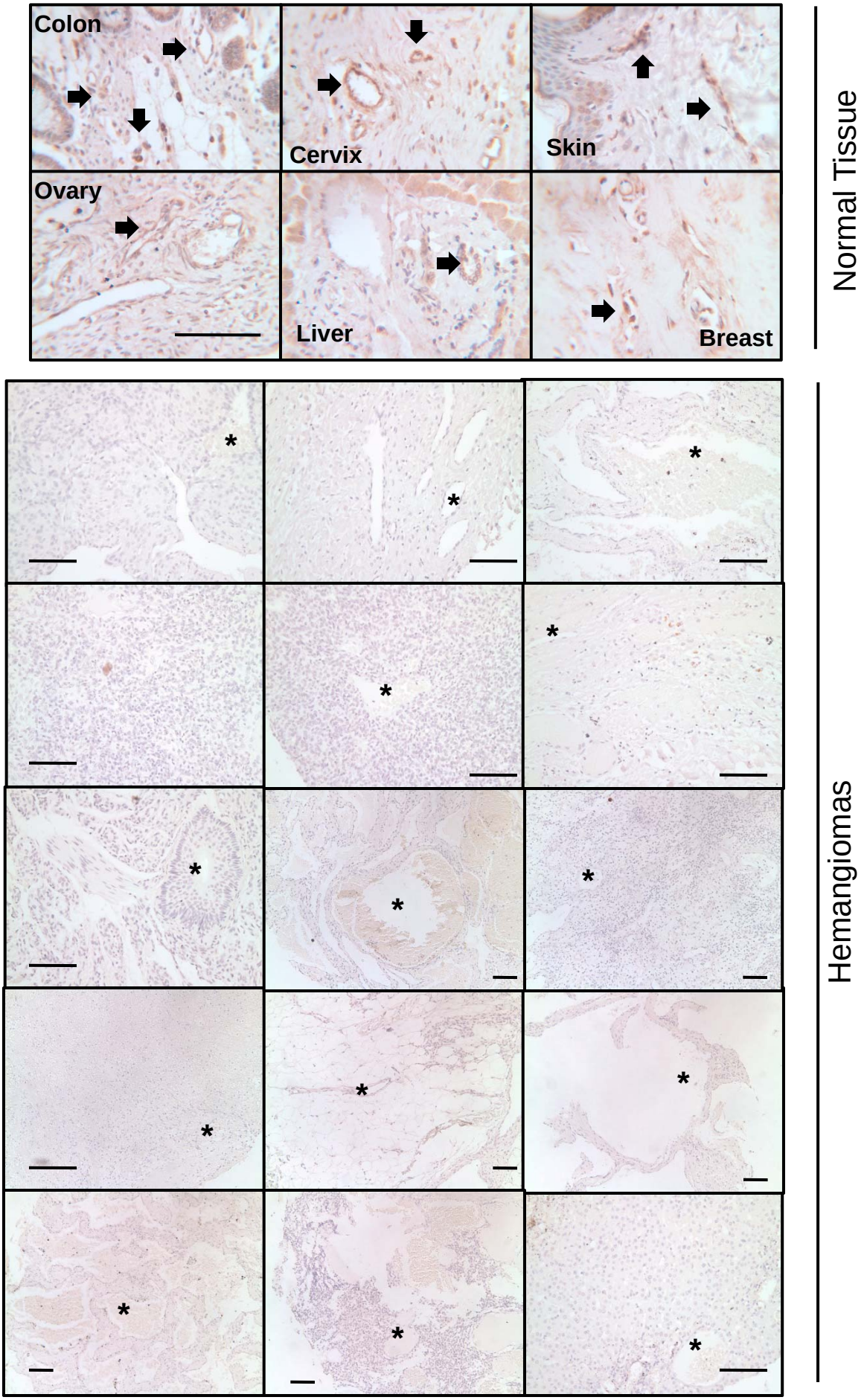

Nature Medicine: doi:10.1038/nm.2186

b

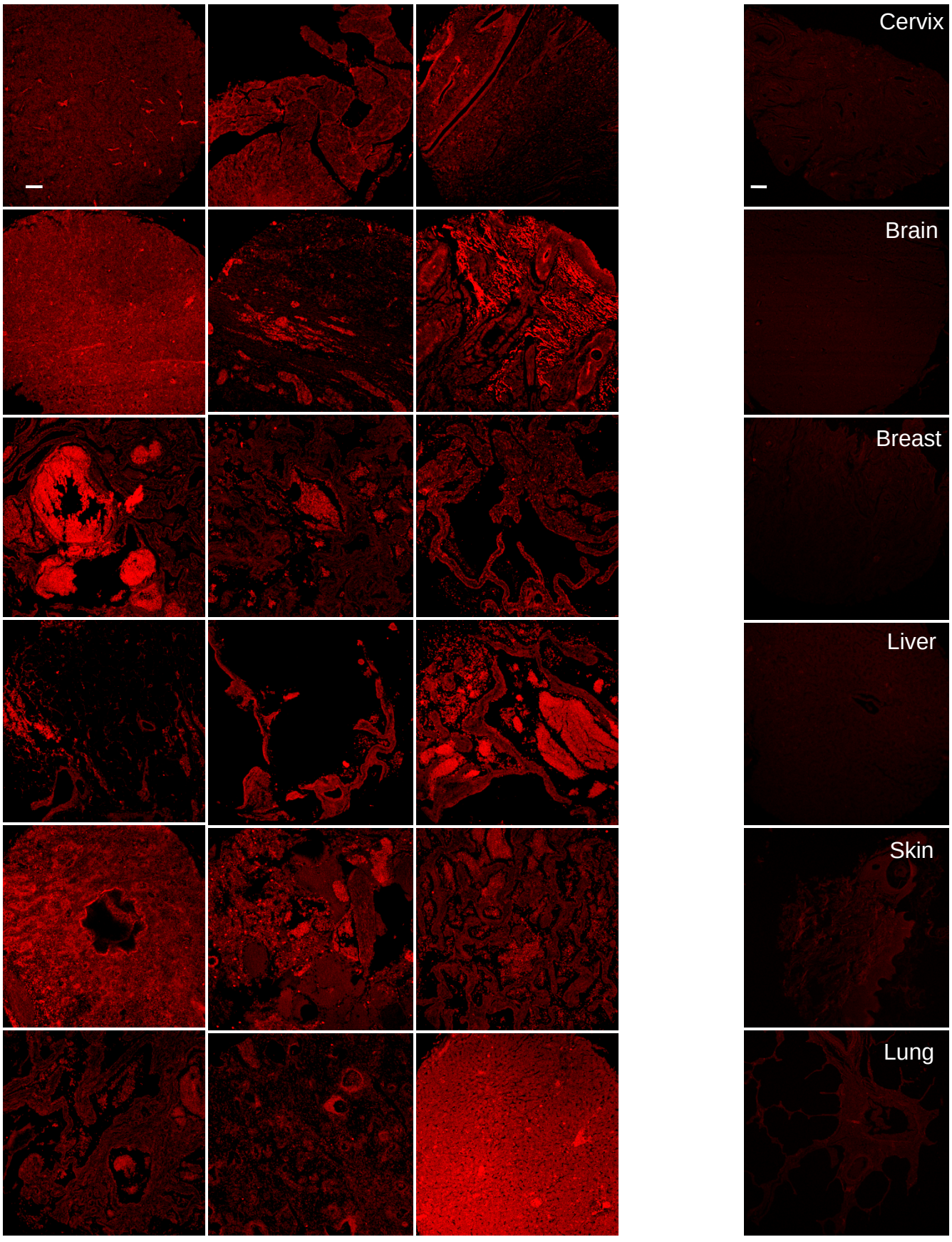

Nature Medicine: doi:10.1038/nm.2186

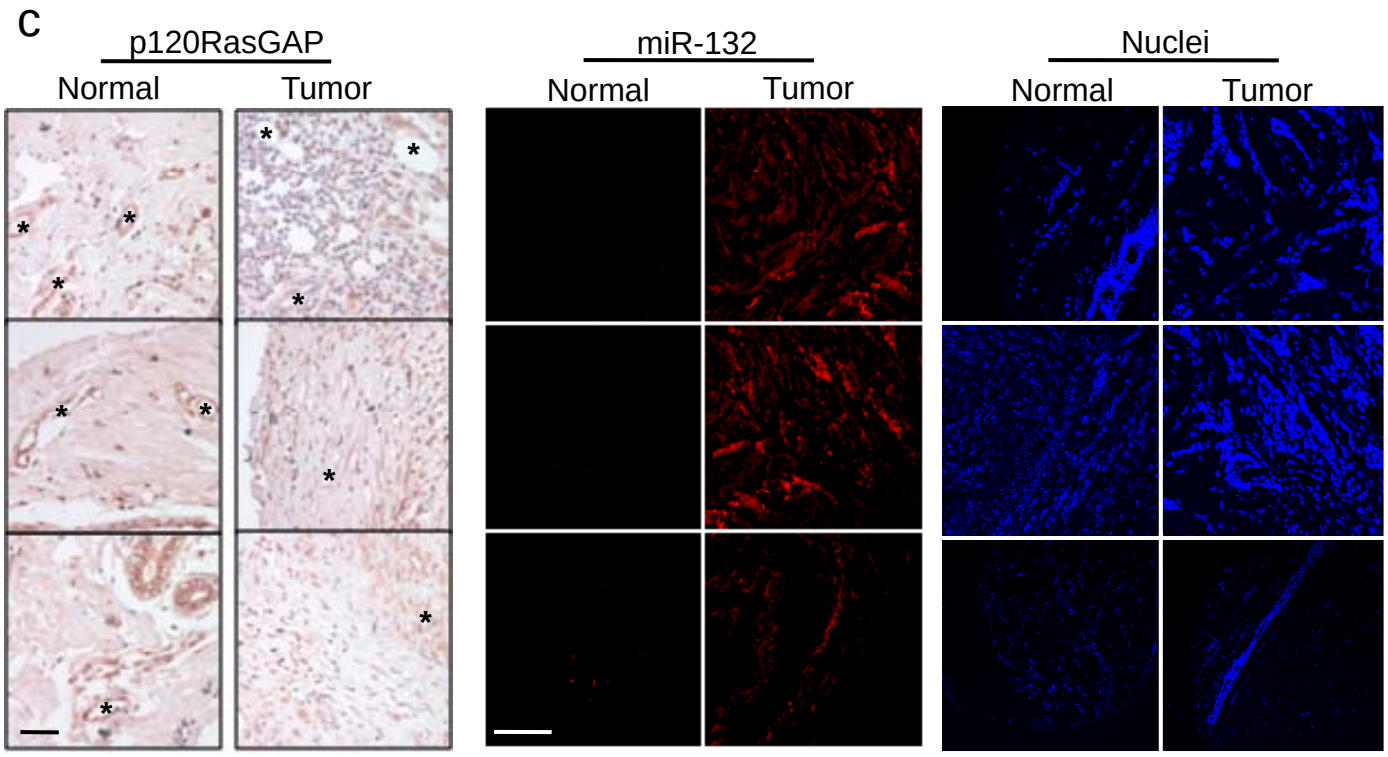

Supplementary Figure 12. Reciprocal expression of miR-132 and p120RasGAP on hyperproliferative hemangiomas but not on the normal endothelium. **(a)** Representative images from immunohistochemical staining for p120RasGAP on normal tissue array and hemangioma array. Arrows indicate blood vessels staining positive and * indicates vessels staining negative for p120RasGAP. Scale bar = 100 microns.**(b)** In-situ hybridization of human hemangioma tissue array or normal human tissue slides. Nuclei stained with TOPRO are pseudo-colored green. Scale bar = 100 microns **(c)** Representative images from immunohistochemical staining for p120RasGAP and **(d)** in situ hybridization for miR-132 on breast tumor and adjacent normal samples from a tissue array. * indicates vessels. Scale bar = 100 microns

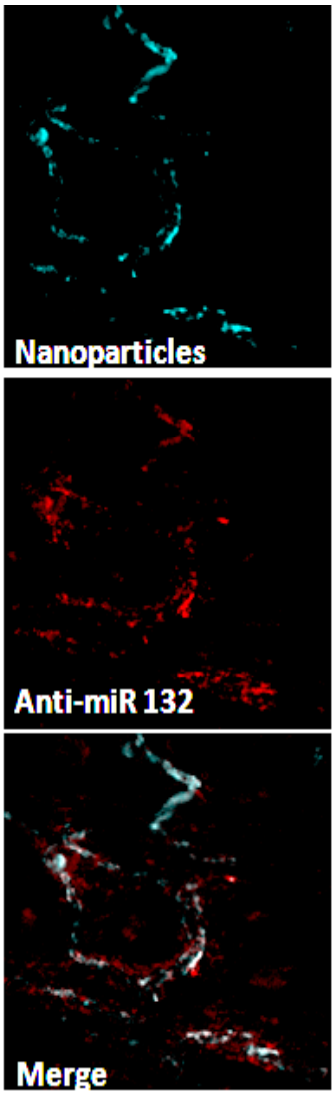

Supplementary Figure 13. Delivery of anti miR-132 using nanoparticles to tumor vasculature. Nude mice were injected subcutaneously with $2x10^6$ M21 human melanoma cells. 14 days later mice were injected i.v with BODIPY labeled RGD-nanoparticles containing Cy-3 labeled anti-miR-132. The mice were euthanized 6 hours later and the tumors were harvested, sectioned and imaged using confocal microscopy.

a

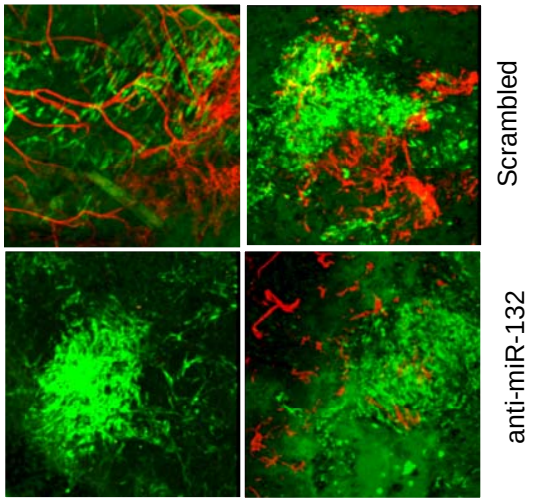

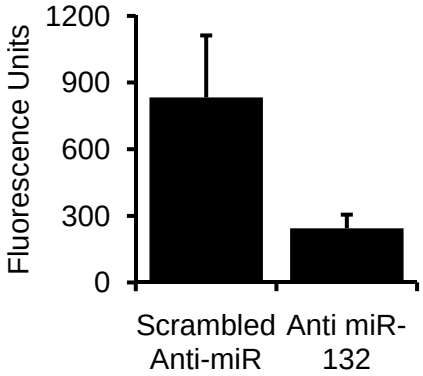

b

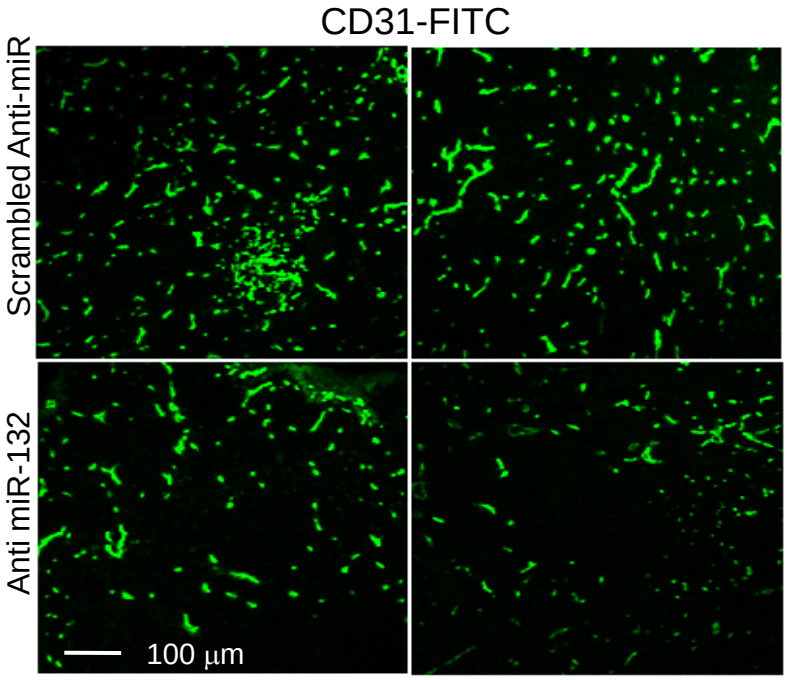

Supplementary Figure 14. Targeted delivery of anti-miR-132 decreases angiogenesis in tumors. a) C57BL/6 mice were injected subcutaneously with 50,000 VEGF-expressing, GFP+, ID-8 ovarian carcinoma cells in matrigel. Two days later, treatment was initiated with either 10 μg scrambled anti-miR or anti-miR-132 in RGD-nanopartcles and repeated every two days. On day 10 the mice were injected with Alexafluor-647 lectin, euthanized, plugs were harvested, lysed in RIPA and the lectin content was quantified on a spectrophotometer (right panel). Bars show mean + s.e.m of atleast 4 mice per group. Scale bar = 100 microns. **b)** Nude mice were implanted with 2 x 10^6 MDA-MB 231 cells in the mammary fat pad. 8 days later, the tumors were measured and mice with palpable tumors of similar volumes were randomly assigned to three groups. Mice received 50 μg of scrambled anti-miR or anti-miR-132 every 48 hours until day 24. Representative images from sections stained for CD31 expression are shown.

a

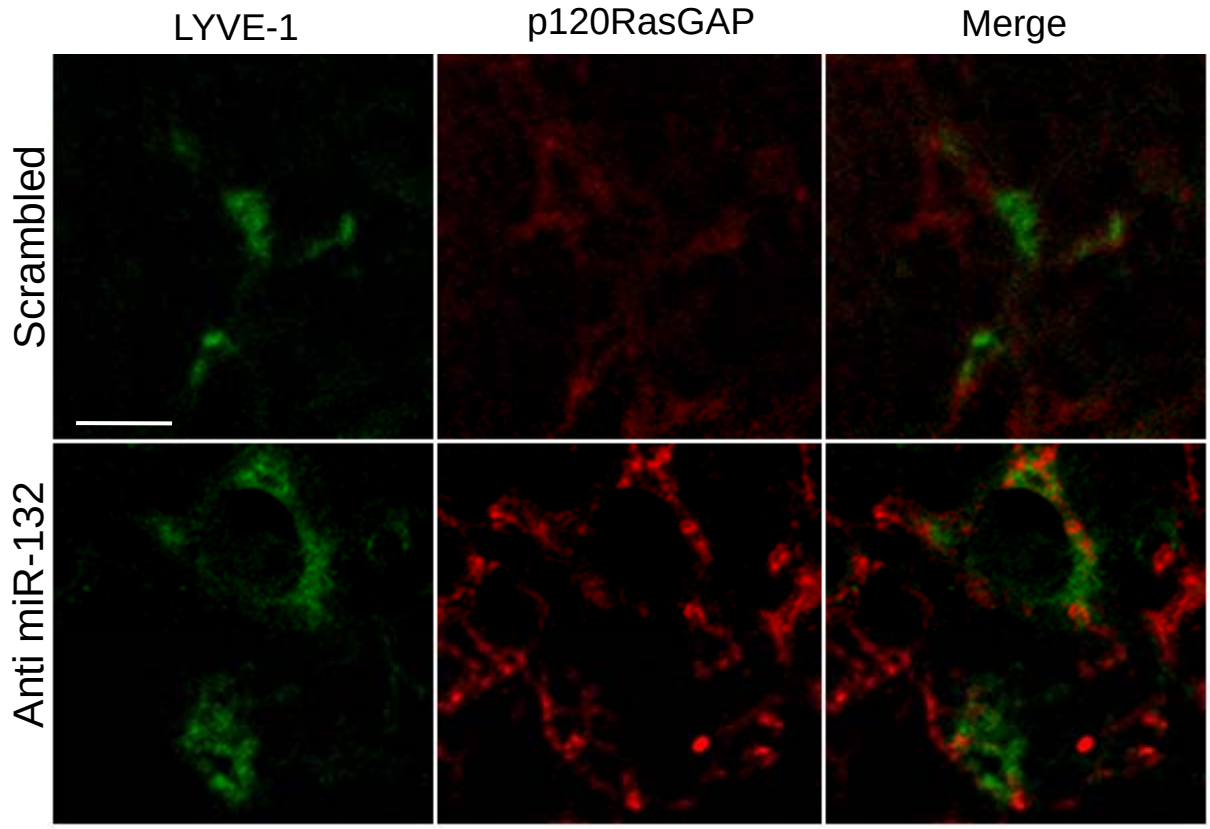

b

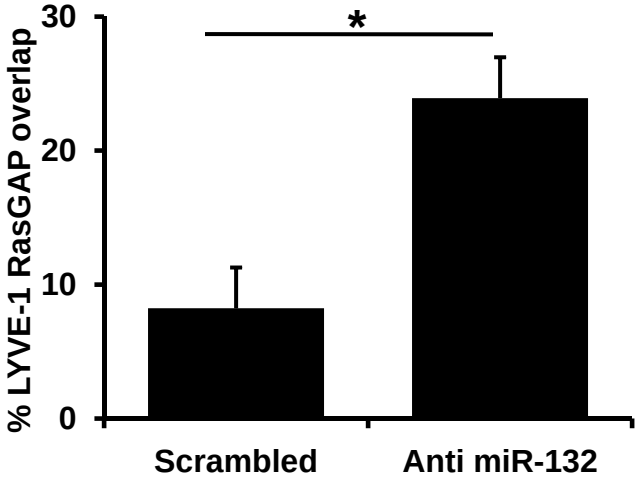

Supplementary Figure 15. Anti miR-132 upregulates expression of p120RasGAP in LYVE1 positive cells. Nude mice were implanted with 2 x 10^6 MDA-MB 231 cells in the mammary fat pad. 8 days later, the tumors were measured and mice with palpable tumors of similar volumes were randomly assigned to treatment groups receiving either 50 μg of scrambled anti-miR or anti-miR-132 every 48 hours until day 24. Tumor sections were stained for LYVE-1 and p120RasGAP expression **(a)** and the LYVE1 p120RasGAP colocalization was quantified using Metamorph **(b)**. Scale bar = 100 microns. Bars show mean + s.e.m of 3 sections from atleast 3 mice per group

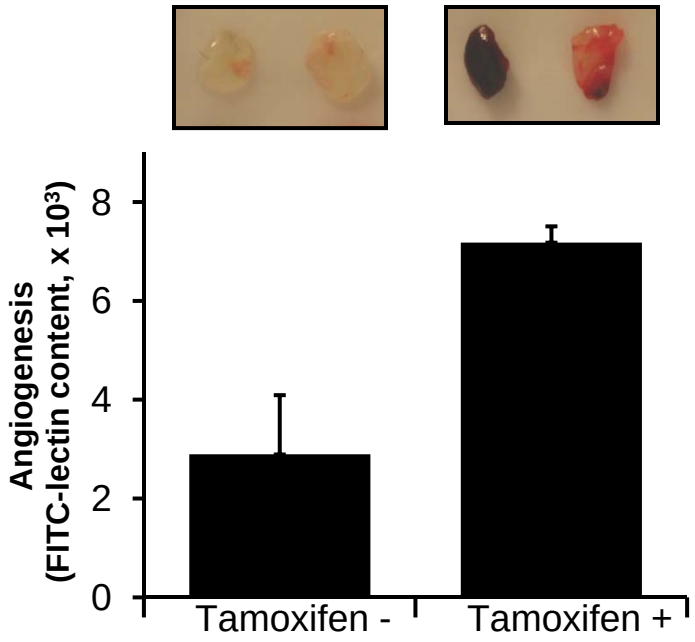

Supplementary Figure 16. Deletion of p120RasGAP increases the angiogenic response to bFGF in Matrigel plugs. p120RasGAP$^{fl/fl}$ Cre^{+} mice were left untreated or treated with Tamoxifen (2mg/mouse in corn oil) every three days for a total of nine days. They were then implanted with subcutaneous matrigel plugs containing bFGF. Five days later, the mice were injected with FITC-lectin and the plugs were harvested, homogenized and the lectin content was quantified. Bars show mean+ s.e.m of atleast 3 plugs per group.

Nature Medicine: doi:10.1038/nm.2186